PCCP

H/D isotope effects on the low-temperature NMR parameters and hydrogen bond geometries of $(FH)_2F^-$ and $(FH)_3F^-$ dissolved in CDF_3/CDF_2Cl†

Ilya G. Shenderovich,[ab] Hans-Heinrich Limbach,*[a] Sergei N. Smirnov,[b] Peter M. Tolstoy,[ab] Gleb S. Denisov*[b] and Nikolai S. Golubev*[b]

[a] *Institut für Chemie der Freien Universität Berlin, Takustrasse 3, D-14195, Berlin, Germany. E-mail: limbach@chemie.fu-berlin.de; Fax: +49 30 8385 5310; Tel: +49 30 8385 5375*

[b] *Institute of Physics, St. Petersburg State University, 198504, St. Petersburg, Russian Federation. E-mail: NMR@paloma.spbu.ru*

Received 1st July 2002, Accepted 9th September 2002
First published as an Advance Article on the web 18th October 2002

Using liquid state ^1H, ^2H and ^{19}F NMR spectroscopy in the temperature range 110–130 K we have studied the hydrogen-bonded anions $(FH)_2F^-$ and $(FH)_3F^-$ and their partially and fully deuterated analogs dissolved in the low-freezing freon mixture CDF_3/CDF_2Cl, in the presence of $(C_4H_9)_4N^+$ as the counter cation. The spin multiplets of the three isotopologs HH, HD, DD of $(FH)_2F^-$, and of the four isotopologs HHH, HHD, HDD, DDD of $(FH)_3F^-$ have been resolved and assigned. Thus, we were able to determine the zero-, one- and two-bond H/D isotope effects on the hydrogen and fluorine NMR chemical shifts as well as isotope effects on the scalar spin–spin hydrogen–fluorine and fluorine–fluorine coupling constants. Using the valence bond order model these NMR data are related to H/D isotope effects on the hydrogen bond geometries. A semi-quantitative interpretation of the observed long range isotope effects is proposed in terms of an anti-cooperative coupling between the hydrogen bonds within each anion. The experimental data can be rationalized in terms of an empirical NMR isotope sum rule, which is analogous to a similar rule for the vibrational frequencies.

Introduction

Intrinsic H/D isotope effects on NMR chemical shifts are caused by the dependence of chemical shielding on the nuclear coordinates which are altered by isotopic substitution *via* changes of the molecular vibrational wave functions. These effects can provide useful information about molecular potential energy surfaces[1–3] and are widely used in the studies of strong hydrogen bonding. In particular, the sign of zero-bond (or primary) isotope effect, *i.e.*, the difference between the deuteron and proton hydrogen bond chemical shifts, provides information about the single- or double-well character of the potential function describing the proton motion.[4–8] One-bond isotope effects on the ^{15}N NMR chemical shifts have been connected to the proton locations in hydrogen-bonded systems of the N···H···N type.[9] On the other hand, long-range ^{13}C isotope shifts have been rationalized in terms of proton transfer equilibria, *e.g.* O–H···N ⇄ O$^-$···H–N$^+$ in the intramolecular hydrogen bond.[10,11] At present, the theory of NMR isotope effects for simple molecules based on quantum mechanical calculations of nuclear shieldings and scalar spin–spin coupling constants as functions of internal vibrational coordinates is well developed[1–3,12–22] and can be extended to isotopologs of hydrogen-bonded complexes.[23]

Most experimental data on NMR isotope effects refer to molecules with intramolecular hydrogen bonds, which are often too complicated for a high-level quantum mechanical calculation. Further information can be obtained by measuring ^3H isotope effects on the chemical shifts of compounds tritiated at the hydrogen bond sites.[7,8] A great problem is that NMR studies of intermolecular hydrogen-bonded systems in solution are hindered by fast proton and hydrogen bond exchange. Therefore, there are only very few experimental data which are suitable for comparison with quantum mechanical calculations. NMR experiments using liquefied low-freezing freon mixtures such as CDF_3/CDF_2Cl can be performed at temperatures as low as 90–150 K, and allow one to record spectra of various hydrogen-bonded systems in the slow exchange regime. In this regime a well resolved fine structure arising from magnetic non-equivalency, scalar spin–spin coupling and isotopic substitution can be observed.[15,24–28]

Using this low-temperature technique, we have shown that it is also possible to measure so-called "vicinal" isotope effects on NMR parameters of a given intermolecular hydrogen bond caused by isotopic H/D substitution of a neighbouring hydrogen bond.[26–28] These effects can provide information on the coupling of several hydrogen bonds in a complex molecular system.

The scope of this study was to measure H/D isotope effects on the NMR parameters of the anionic clusters $(FH)_nF^-$, $n = 2,3$, which have been observed recently in CDF_3/CDF_2Cl with $(C_4H_9)_4N^+$ as counter cation.[25a] The H/D isotope effects for the anion $(FHF)^-$ have been described previously.[6,29] These anions are especially interesting as, for the first time, large scalar couplings between all nuclei of a hydrogen bridge were observed and verified by quantum mechanical calculations using DFT methods,[25a] and also using coupled cluster calculations.[30] As these systems represent the simplest type of strongly coupled hydrogen bonds, they can also serve as models of hydrogen-bond coupling

† Presented at the annual meeting of the Deutsche Bunsen-Gesellschaft für Physikalische Chemie, Potsdam, Germany, May 9–11, 2002.

 DOI: 10.1039/b206323a

for more complicated hydrogen-bonded chains of biological interest.

This paper is organized as follows. After an experimental section the results are presented and discussed. In particular, we show that a simple isotope sum rule of the type established previously for vibrational frequencies of isotopologs of free molecules seems to be valid in the case of NMR parameters of hydrogen-bonded complexes.

Experimental

Solutions of the salts $(C_4H_9)_4N^+(FH)_nF^-$, with $n = 2,3$ and their deuterated analogs were prepared by a modification of a procedure described previously.[25a] In the first step, crystalline $(C_4H_9)_4N^+F^-\cdot H_2O$ (TBAF, Aldrich) was dried by repeated azeotropic distillation with dichloromethane and weighed. Then 40% hydrofluoric acid was added and the water removed again by azeotropic distillation with dichloromethane. The residual oil contains three tetrabutylammonium salts, with $(FHF)^-$, $(FH)_2F^-$, $(FH)_3F^-$ and, presumably, $(FH)_4F^-$ as counter anions.[25a] The ratio of the ions depends strongly on the amount of hydrofluoric acid added. Deuteration of the anions was performed by repeatedly dissolving the salt mixtures in CH_3OD and removing the solvent under vacuum. All the chemical operations were performed using Teflon flasks in order to prevent reaction with the silica glass surface. The resulting oil was placed into an NMR glass sample tube (Wilmad, Buena) equipped with a Teflon valve which could be attached to a vacuum line. In a subsequent step, the tube was filled by vacuum transfer with low-freezing solvent mixtures of CDF_3/CDF_2Cl prepared and dried as described previously.[15,24,25] During the synthesis of the deuterated freon mixture it is difficult to control conditions precisely in order to get the mixture of a given composition, so from synthesis to synthesis the solvent composition could change within the 1:1–1:5 range, estimated from the intensity of the residual ^1H NMR solvent signals.[31] The samples were subsequently stored at 77 K to avoid reactions with glass prior to the NMR measurements. NMR spectra were recorded in the temperature range 110–130 K using a Bruker AMX-500 instrument operating at 500 MHz. ^1H, ^2H and ^{19}F chemical shifts were measured using fluoroform, CHF_3 (CDF_3), as internal standard, and converted to the conventional scales, TMS and $CFCl_3$.

As has been demonstrated previously, the composition of the freon mixture and the sample temperature determine the polarity of the solvent and can affect the geometry of hydrogen-bonded complexes and hence their NMR chemical shifts.[31]

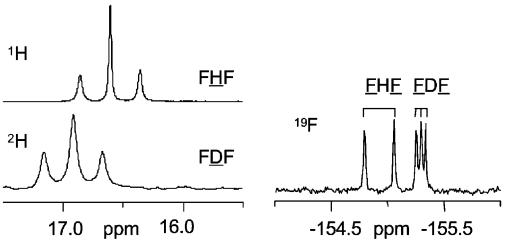

Fig. 1 ^1H, ^2H and ^{19}F NMR spectra of a solution containing partially deuterated tetrabutylammonium hydrogen (deuterium) bifluoride in CDF_3/CDF_2Cl at 130 K. The deuterium fraction in the mobile proton sites was about $x_D \approx 0.5$.

In this study, however, we did not observe significant changes in the NMR parameters of $(FH)_2F^-$ and $(FH)_3F^-$ clusters induced by moderate changes in the absolute sample concentration and solvent composition at a given temperature. Nevertheless, estimations of the salt concentrations were obtained by weighing the initial amount of added TBAF, and by measuring the volume of the solutions in the calibrated NMR tubes around 120 K. Approximate concentrations were of the order of 0.02 M.

Results

As reported previously,[25a] in solutions of FH and TBAF in liquefied freons various hydrogen-bonded complexes of the type $(FH)_nF^-$ are formed with $n = 1$ to 4, whose relative concentrations depend on the FH/TBAF ratio. A short account on the complex with $n = 1$ was given recently.[6] Here, we studied mainly samples with $n = 2$ and 3 as main constituents, as a function of the deuterium fraction x_D in the mobile proton sites, leading to the formation of all possible isotopologs $(FL)_2F^-$ and $(FL)_3F^-$, with L = H, D.

The NMR signals of all species with $n = 1$ to 3 recorded at 130 K are depicted in Figs. 1 to 4, and the NMR parameters obtained are assembled in Tables 1 to 3. We note already here that the parameters of $(FH)_2F^-$ and $(FH)_3F^-$ compare well with those obtained previously;[25a] they are little dependent on temperature and concentration. As they were obtained in this study to a large extent by line shape analysis we think that their precision is increased. In the following, we will first describe the signals of the non-deuterated anions and then the effects of deuteration.

Fig. 1 contains the low-temperature NMR signals of FHF^- and FDF^-. As expected, they are split by scalar coupling with

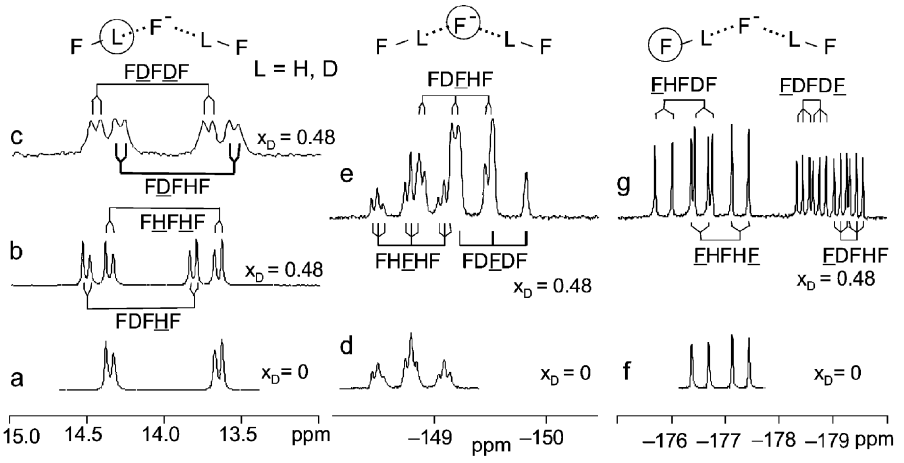

Fig. 2 ^1H, ^2H and ^{19}F NMR spectra of a solution containing partially deuterated tetrabutylammonium dihydrogen (deuterium) trifluoride in CDF_3/CDF_2Cl at 130 K. The spectra a, d and f come from a sample containing no deuterium. The spectra b, c, e and g come from a sample containing about 50% of deuterium in the hydrogen bonds ($x_D \approx 0.5$).

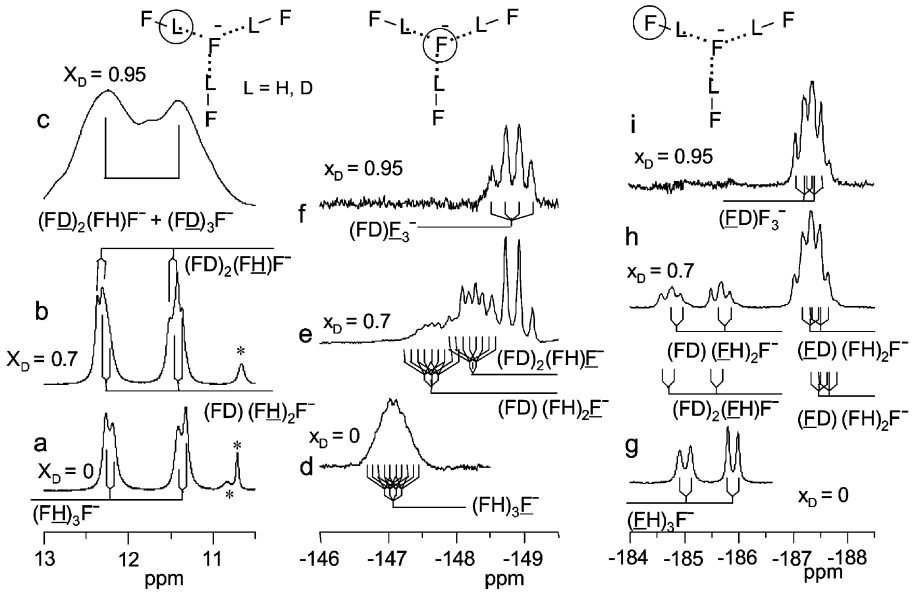

Fig. 3 ^{19}F NMR spectra of solutions containing partially deuterated tetrabutylammonium trihydrogen (deuterium) tetrafluoride in CDF_3/CDF_2Cl at 130 K. The spectra a, d and g come from a sample containing no deuterium. The spectra b, e and h come from a sample with $x_D = 0.7$ and c, f and i from a sample with $x_D = 0.95$. Signals marked with * correspond to the unknown HF species.

a normal ratio of J_{FH}/J_{FD}. A primary low-field shift $\delta(FDF) - \delta(FHF) = 0.32$ ppm and a secondary high-field fluorine shift $\delta(FDF) - \delta(FHF) = -0.37$ ppm are observed. These values are independent of temperature in the range 110–170 K, and they are almost identical to those obtained previously[12,29] for acetonitrile solution between 250 and 300 K.

The low-temperature ^{1}H and ^{19}F signals of $(FH)_2F^-$ which are depicted in Fig. 2a, d, and f are in agreement with those described previously;[25a] the main features are the large coupling J_{FF} and the couplings $J_{H\cdot\cdot F}$ across the hydrogen bond. The signal pattern can be described in good approximation in terms of an A_2M_2X spin system, with a triplet of triplets for the central fluorine, and a doublet of doublets for the two external fluorines and for the two protons. The largest coupling is J_{FH}; J_{FF} is the second in size and $J_{H\cdot\cdot F}$ the smallest. As discussed previously,[25a] the observation of a larger line width of the inner signal components in Fig. 2a indicates that the sign of the latter is negative. This finding has been confirmed by DFT[25a] and coupled cluster calculations.[30] Three-bond couplings J_{FH} or two-bond couplings J_{HH} are not resolved; they would lead to a high-order AA′MM′X spin system. As has been argued previously,[25a] the spin–spin splitting patterns of this species prove the chemical structure of the anion as a fluoride ion cluster with two HF molecules, $FH\cdots F^-\cdots HF$, in agreement with the available theoretical and experimental data.[30,32–35]

The ^{1}H and ^{19}F signals of the $(FH)_3F^-$ anion are depicted in Fig. 3a, d, and g. They are similar to those of the $(FH)_2F^-$ anion, with the exception that the ^{19}F signal of the central fluorine nucleus is a poorly resolved quartet of quartets, instead of a triplet of triplets for $(FH)_2F^-$, due to the scalar spin coupling with three equivalent ^{1}H and three equivalent ^{19}F nuclei. Thus, this anion constitutes a first-order A_3M_3X spin system. Note that by chance, $J_{H\cdot\cdot F} \approx \frac{1}{2} J_{FF}$; this circumstance leads to an apparently simplified signal pattern of the terminal fluorine signals. The above findings confirm a star-like structure with the central fluoride ion taking part in three hydrogen bonds with HF molecules, in accordance with the our previous data[25a] and results.[32–35] As depicted in Figs. 2 and 3, partial deuteration of the salts results in additional lines arising from the occurrence of the isotopologs $(FL)_2F^-$ and $(FL)_3F^-$ (L = H, D). Their assignment is straightforward and was assisted by varying the deuterium fraction x_D in the mobile proton sites. We note that in all cases the signal patterns remained of first order. The ^{19}F signal patterns correspond to those expected when the doublet splittings arising

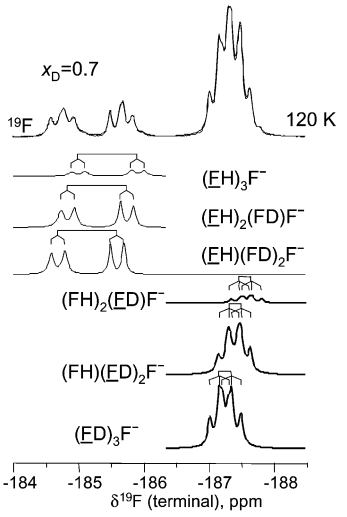

Fig. 4 Upper trace: superposed simulated and experimental part of the spectrum of Fig. 3h. The lower traces show the various line components arising from the HHH, HHD, HDD and DDD isotopologs of the $(FH)_3F^-$ anion.

Table 1 NMR parameters of the H,D isotopologs of hydrogen bifluoride anion as a tetrabutylammonium salt in a freon mixture at 130 K

	FHF^-	FDF^-
Point group	$D_{\infty h}$	$D_{\infty h}$
$\delta(FLF)$/ppm (±0.005)	16.60	16.92
$\delta(FLF)$/ppm (±0.01)	−154.96	−155.33
J_{FL}/Hz (±0.5)	124.0	19 (124)[a]
$K_{FL}/10^{20}$ T^2 J^{-1} (±0.005)[b]	1.097	1.095

[a] The value converted to the proton scale, (γ_H/γ_D) J is given in parentheses. [b] Reduced coupling constant $K_{XY} = 4\pi^2/h \cdot J_{XY}/\gamma_X/\gamma_Y$.

Table 2 NMR parameters of three H,D isotopologs of the dihydrogen trifluoride anion as a tetrabutylammonium salt in a freon mixture at 130 K

	$FHFHF^-$	$FHFDF^-$	$FDFDF^-$	$\Delta = (V(HH) + V(DD)) - (V(HD) + V(DH))$
Point group	C_{2v}	C_s	C_{2v}	
$\delta(F\underline{H}FLF)$/ppm (±0.005)	14.015	14.170	—	
$\delta(F\underline{D}FLF)$/ppm (±0.005)	—	13.930	14.090	0.005 (2%)[a]
$\delta(\underline{F}HFLF)$/ppm (±0.005)	−176.900	−176.225	—	
$\delta(\underline{F}DFLF)$/ppm (±0.005)	—	−179.305	−178.615	0.015 (0.5%)[a]
$\delta(FL\underline{F}LF)$/ppm (±0.02)	−148.75	−149.16	−149.52	0.05 (7%)[a]
J_{FH}/Hz (±0.5)	354.3	347.9	—	
J_{FD}/Hz (±0.5)	—	57.3 (373)[b]	56.0 (365)[b]	−1.6 (6%)[a]
$K_{FH}/10^{20}$ T^2 J^{-1} (±0.005)[c]	3.137	3.077	—	
$K_{FD}/10^{20}$ T^2 J^{-1} (±0.005)[c]	—	3.302	3.227	
$J_{F(H)F}$/Hz (±0.5)	146.5	151.1	—	
$J_{F(D)F}$/Hz (±0.5)	—	139.9	143.9	−0.6 (5%)[a]
$K_{F(H)F}/10^{20}$ T^2 J^{-1} (±0.005)[c]	1.377	1.420	—	
$K_{F(D)F}/10^{20}$ T^2 J^{-1} (±0.005)[c]	—	1.315	1.352	
$J_{H\cdot\cdot F}$/Hz (±0.5)	−24.5	−22.7	—	
$K_{H\cdot\cdot F}/10^{20}$ T^2 J^{-1} (±0.005)[c]	−0.217	−0.201	—	

[a] V: parameter according to first column. % with respect to the largest isotope effect in parentheses. [b] Values converted to the proton scale, (γ_H/γ_D) J in parentheses. [c] Reduced coupling constant $K_{XY} = 4\pi^2/h \cdot J_{XY}/\gamma_X/\gamma_Y$.

from coupling with ^{1}H are replaced by triplets arising from coupling with ^{2}H, taking into account that $J_{FH}/J_{FD} = \gamma_H/\gamma_D = 6.514$. Unfortunately, we did not succeed in resolving the coupling constants $J_{D\cdot\cdot F}$ across the hydrogen bond for either of the two anions.

The ^{1}H and ^{2}H signal patterns of $(FL)_2F^-$ are well resolved (Fig. 2b, c). We note a displacement of the central fluorine chemical shift to higher fields when H is replaced successively by D (Fig. 2e). The chemical shifts of the terminal fluorines are increased by replacement of H by D when the substitution occurs in the neighbouring H-bond, otherwise the shifts are decreased (Fig. 2g). As depicted in Fig. 3b, c, e, f, h and i, similar features are observed for $(FL)_3F^-$, although a strong signal overlap makes a visual assignment difficult.

To evaluate the spectroscopic parameters of the isotopologs, a computer simulation of the spectra was performed using the approximation of the superposition of first order spin multiplets. Chemical shifts and spin–spin coupling constants and also the widths of the individual lines were obtained by adapting the simulated to the experimental spectra. An example of the deconvolution of multiplets belonging to different isotopologs is given in Fig. 4. The parameters obtained are included in Tables 1 to 3.

Discussion

We have succeeded in measuring H/D isotope effects on the chemical shifts and coupling constants of FLF^-, $(FL)_2F^-$ and $(FL)_3F^-$ (L = H, D) in freon solution by low-temperature NMR. To our knowledge, with the exception of FLF^-,[6] data of this kind have not been reported previously; they may be valuable in the future as input for quantum mechanical calculations of the hydrogen bond structure of hydrogen-bonded complexes or clusters. In the following we will (i) shortly review H/D isotope effects on single and coupled H-bonds as discussed previously, (ii) review and complete the connection between the NMR parameters and the hydrogen bond geometries of $(FL)_nF^-$ clusters, which will allow us to

Table 3 NMR parameters of four H,D isotopologs of trihydrogen tetrafluoride anion as a tetrabutylammonium salt in a freon mixture at 130 K

	$F(HF)_3^-$	$F(HF)_2(DF)^-$	$F(HF)(DF)_2^-$	$F(DF)_3^-$	$\Delta = (V(HHH) + V(DDD)) - (V(HHD) + V(HDD))$
Point group	D_{3h}	C_{2v}	C_{2v}	D_{3h}	
δ(H)/ppm (±0.01)	11.79	11.84	11.89	—	0.04 (25%)[a]
δ(D)/ppm (±0.03)	—	11.74	11.81	11.88	
δ(F(H))/ppm (±0.02)	−185.50	−185.35	−185.19	—	0.00 (0%)[a]
δ(F(D))/ppm (±0.02)	—	−187.62	−187.44	−187.31	
$\delta(F^-)$/ppm (±0.04)	−147.08	−147.65	−148.24	−148.82	0.01 (1%)[a]
J_{FH}/Hz (±2)	430	428	427	—	—
J_{FD}/Hz (±2)	—	67 (436)[b]	67 (436)[b]	67 (436)[b]	
$K_{FH}/10^{20}$ T^2 J^{-1} (±0.02)[c]	3.80	3.79	3.78	—	
$K_{FD}/10^{20}$ T^2 J^{-1} (±0.02)[c]	—	3.86	3.86	3.86	
$J_{F(H)F}$/Hz (±2)	94	97	97	—	—
$J_{F(D)F}$/Hz (±2)	—	90	92	92	
$K_{F(H)F}/10^{20}$ T$^{2\ -1}$ (±0.02)[c]	0.88	0.91	0.91	—	
$K_{F(D)F}/10^{20}$ T^2 J^{-1} (±0.02)[c]	—	0.85	0.86	0.86	
$J_{H\cdot\cdot F}$/Hz (±2)	−45	−45	−47	—	—
$K_{H\cdot\cdot F}/10^{20}$ T^2 J^{-1} (±0.02)[c]	−0.40	−0.40	−0.42	—	

[a] V: parameter according to first column. % with respect to the largest isotope effect in parentheses. [b] The values converted to the proton scale, (γ_H/γ_D) J in parentheses. [c] Reduced coupling constant $K_{XY} = 4\pi^2/h \cdot J_{XY}/\gamma_X/\gamma_Y$ in parentheses.

(iii) discuss the isotope effects on NMR parameters obtained in this study in terms of geometric H/D isotope effects.

Geometric H/D isotope effects on hydrogen bonds

The problem of H/D isotope effects on hydrogen bond geometries in the absence of proton tautomerism has been studied in various theoretical[7,12,14,36a] and experimental papers.[9,26,27,36b,36c,37] The main results are visualized in Fig. 5. Firstly, we note that one can characterize the average positions of the hydrogen bond atoms by the average distances $q_1 = \frac{1}{2}(r_1 - r_2)$ and $q_2 = r_1 + r_2$, and the average hydrogen bond angle α (Fig. 5a) which is 180° for a linear hydrogen bond. r_1 and r_2 correspond to the two heavy atom–hydrogen distances, q_1 to the deviation of the hydrogen nucleus from the hydrogen bond center. For linear H-bonds with $\alpha = 180°$ q_2 corresponds to the A···B distance. In addition to this point approach, a hydrogen bond is characterized by a particularly large amplitude vibration leading to a substantial delocalization of the hydrogen atom. This effect is visualized in Fig. 5a for the case of an axially symmetric H-bond by distorted ellipsoids characterized by the mean square displacements Δq_1^2 for the delocalization along the strongly anharmonic AH stretching mode and by $\Delta\varphi^2$ for the bending mode. Δq_1^2 and $\Delta\varphi^2$ depend strongly on the symmetry of the hydrogen bond as illustrated schematically in Fig. 5b.

H/D substitution leads to a change in all quantities (Fig. 5b). In the case of a symmetric H-bond the isotope effect $\Delta q_{1D}^2 - \Delta q_{1H}^2 < 0$ indicates that D is confined more to the H-bond center than H. On the other hand, $q_{1D} - q_{1H} = 0$, but $q_{2D} - q_{2H}$ can be slightly negative. In the case of an asymmetric H-bond the main features are that the "covalent" bond becomes shorter and the "H-bond" longer, *i.e.* $|q_{1D} - q_{1H}| \neq 0$. Because of the H-bond correlations discussed later, the value q_2 is generally increased upon deuteration. Here the changes in the quadratic terms are less important.

For the coupled hydrogen bonds one can distinguish two types of isotope effects, *i.e.* "direct" isotope effects similar to those discussed above for single H-bonds and "vicinal" isotope effects arising from H/D substitution in a neighbouring coupled H-bond.[26,28] Vicinal isotope effects depend on whether the coupled hydrogen bonds are "cooperative" or "anti-cooperative". In the former, H/D-substitution in a given bond leads to similar effects in the neighbouring bond, whereas in the latter the effects in both bonds are opposite as illustrated schematically in Fig. 5c and d.

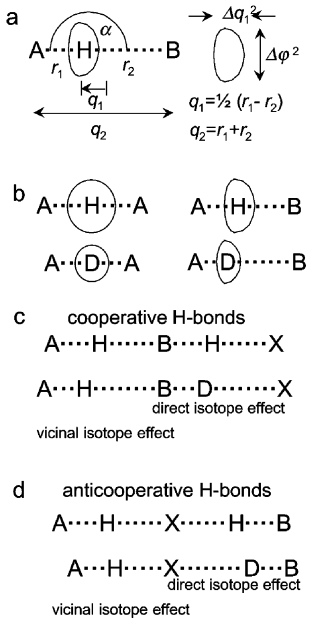

Fig. 5 Schematic illustration of (a) main geometric parameters of a single hydrogen bond, (b) of H/D isotope effects in single symmetric and asymmetric hydrogen bonds, (c) of cooperatively coupled and (d) of anti-cooperatively coupled hydrogen bonds.

The rest of this section is divided into two parts. In the first part we will discuss the relation between hydrogen bond properties and NMR parameters of the complexes studied and in the second part the hydrogen bond H/D isotope effects.

Hydrogen bond correlations in $(FH)_nF^-$ clusters

In this section, we discuss relations of the NMR parameters with the hydrogen bond coordinates q_1 and q_2, without taking into account explicitly the quadratic terms Δq_1^2 and $\Delta\varphi^2$. The basis for this approach is the geometric hydrogen bond correlations observed by neutron crystallography[38] and NMR for OHO, NHN and NHO hydrogen bonds.[9,25] These correlations are derived, in turn, from the valence bond orders p which can be written for FHF^- hydrogen bonds in the following way:

$$p_{FH} = \exp\{-(r_1 - r^\circ)/b\},\ p_{HF} = \exp\{-(r_2 - r^\circ)/b\},\ p_{FH} + p_{HF} = 1, \quad (1)$$

where r° corresponds to the F···H distance in free HF, b is a parameter which describes the bond order decrease with increasing distance. The sum of the two bond orders is unity. Therefore, r_1 and r_2 or q_1 and q_2 are correlated,[25b] *i.e.*

$$q_2 = r_1 + r_2 = 2r^\circ + 2q_1 + 2b\ln[1 + \exp\{-2q_1/b\}]. \quad (2)$$

In the case of the NHN-hydrogen bonds of the C≡N···H···N≡C$^-$ Li^+ system, eqn. (2) has been verified by *ab initio* calculations,[9] which produce the isotope independent equilibrium distances and subsequent calculations for the anharmonic stretching vibrations, which provided the H/D isotope effects on q_1 and q_2. In rough approximation, it was found that the vibrational corrections which are larger for H than for D, shift the data points on the correlation curve. With the exception of the symmetric complex, the deuterated H-bonds generally exhibit larger q_1 values than the protonated H-bonds.

In order to obtain the values of r_1 and r_2 of the $(FH)_nF^-$ clusters studied we have calculated and reported these values previously[25a] using *ab initio* calculations at the MP2/6-31+G(p,d) level, using the symmetries $D_{\infty h}$, C_{2v}, D_{3h} and T_d for $n = 1$ to 4 in $(FH)_nF^-$, in agreement with the average NMR solution symmetries. Within the margin of error of the calculations, the hydrogen bonds were found to be linear. Unfortunately, we were not able in this study to correct the calculated q_1 and q_2 values for the anharmonic groundstate vibrations, which introduces a systematic error into the analysis as discussed below.

We set up now a formal reaction pathway of proton transfer between fluorines with the hypothetical limiting and intermediate states depicted in Scheme 1. "Free" F^- reacts with one, two or three FL molecules to "free" LF, FL_2^+ or FL_3^{2+}

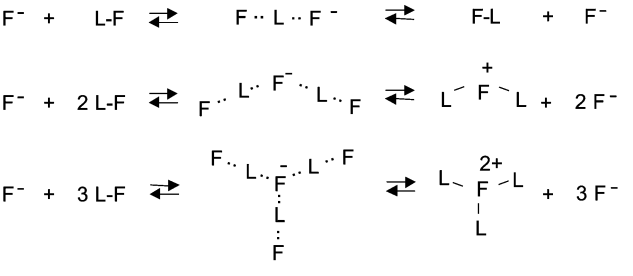

Scheme 1

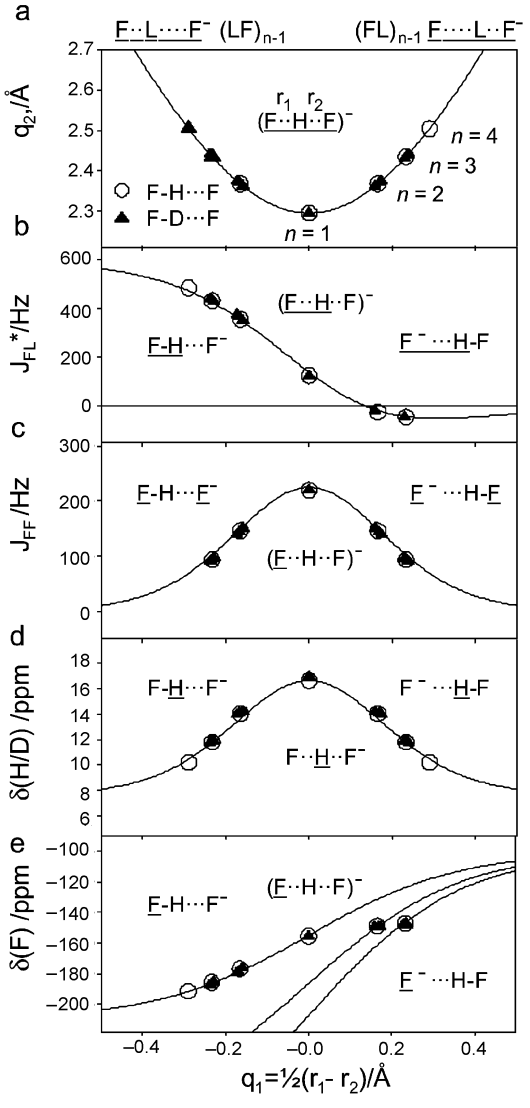

Fig. 6 Correlations of hydrogen bond properties with the coordinate q_1 for the FHF^-, $(FH)_2F^-$, $(FH)_3F^-$ and $(FH)_4F^-$ anions. The values of q_1 were obtained by *ab initio* calculations at the MP2/6-31+G(p,d) level described in ref. 25*a*. (a) calculated heavy atom distance q_2; (b) experimental values of J_{FL}*; (c) experimental values of J_{FF}(the value for FHF^- at $q_1 = 0$ was taken from ref. 30). (d) experimental values of δ^1H (δ^2H); (e) experimental values of $\delta^{19}F$.

and free F^-, *via* hydrogen-bonded clusters $(FL)_nF^-$. Naturally, each complex only adopts a single geometry. On the other hand, the geometries and NMR parameters of the FHF^- units can be represented in single graphs depicted in Fig. 6, where the abscissa represents the deviation q_1 defined in Fig. 5 of the proton from the hydrogen bond center. We define this deviation to be positive when the proton is closer to the central fluorine and negative if the proton is closer to the terminal fluorine nuclei. Thus, the complexes $F(HF)_n^-$ provide a kind of reaction pathway for the transfer of the proton from one fluorine to the other.

In Fig. 6a are plotted the F···F distances, *i.e.* q_2 as a function of q_1. The solid triangles correspond to the calculated equilibrium values. The solid line corresponds to eqn. (2), with the parameters $r^\circ = 0.897$ Å and $b = 0.36$ Å which reproduces well the predicted correlation of the equilibrium values. As the anharmonic vibrational corrections are smaller for the deuterated hydrogen bonds than for the protonated ones, we take the equilibrium values as approximations for the deuterated clusters, as indicated in Fig. 6a. When the hydron (proton, deuteron) is close to the left fluorine, the F···F distance is large but decreases when the hydron is shifted into the hydrogen bond center and increases again when the proton is shifted across the center. The shortest distance of about 2.293 Å is reached in the symmetric bifluoride anion where the F···D distances are 1.147 Å. Eqn. (2) is well fulfilled, and the parameters r° and b were obtained by least squares fitting. We note that the parameters r° and b might need to be adjusted in the future when more sophisticated calculations or experimental data are available.

The data points corresponding to the protonated clusters in Fig. 6a were *not* obtained by *ab initio* calculations, but were obtained *via* the data analysis in Fig. 6b and 6c described in the following. These figures show graphs of the coupling constants as a function of q_1. For a comparison of the fluorine–hydrogen and fluorine–deuterium coupling constants J_{FH} and J_{FD} the trivial effect of the different gyromagnetic ratios γ_L, L = H, D needs to be eliminated. This could be done by discussing the reduced coupling constants K_{FL} to fluorine defined as

$$J_{FH} = \gamma_F\gamma_H K_{FH} h/4\pi^2 \text{ and } J_{FD} = \gamma_F\gamma_D K_{FD} h/4\pi^2 \quad (3)$$

However, we find it more convenient to use the quantities

$$J_{FL}{}^* = J_{FL}\gamma_H/\gamma_L \quad (4)$$

which are plotted in Fig. 6b as a function of q_1. In Fig. 6c are depicted the values of J_{FF}. The solid lines in both figures represent the coupling constant correlations

$$J_{FL}{}^* = J_{FL}{}^{*\circ} p_{FL} - 8\Delta J_{FH}{}^* p_{FL}\, p_{LF}{}^2,\ J_{FL}{}^{*\circ} = 600 \text{ Hz},\ \Delta J_{FH}{}^* = 162.5 \text{ Hz}, \quad (5)$$

$$J_{FF} = J_{FF}{}^\circ (4 p_{FL} p_{FL})^2,\ J_{FF}{}^\circ = 225 \text{ Hz}. \quad (6)$$

which were proposed previously.[25*b*] In the above equations we assume that the same hydrogen bond correlation equations are valid for both the protonated and the deuterated complexes. As we associate the calculated equilibrium values of q_1 to the deuterated clusters, we are then able to determine the q_1 and hence q_2 values of the protonated clusters using the experimental values of J_{FF} and/or of J_{FH} as data input. The data points obtained on the basis of the J_{FF} data are included in Fig. 6 as open circles. However, we note that the data points of the protonated and deuterated clusters are hardly resolved in Fig. 6, which renders a discussion of these effects based on this figure very difficult. Therefore, this first approach to determine the isotope effects on the hydrogen bond geometries was later refined, as described in the next section, and the data points in Fig. 6 refer in fact to the refined values.

The coupling $J_{FL}{}^{*\circ}$ is around 600 Hz and assumed to be the same for both hydrons in the free LF molecule. The coupling J_{FF} across the hydrogen bond is then zero. When L is shifted towards the H-bond center, $J_{FL}{}^*$ decreases because of the decrease in the p_{FH} bond order corresponding to the first term in eqn. (1); however, J_{FF} increases, exhibiting a maximum of about 220 Hz at the shortest F···F distance at $q_1 = 0$. This value cannot be measured directly but was proposed by some of us by extrapolation from the higher $(FL)_nF^-$ clusters.[39] A slightly larger equilibrium value of $J_{FF} = 225$ Hz was calculated recently for FHF^- by Perera *et al.*[30] using very precise CCSD *ab initio* calculations. Therefore, we have included their value in the graph of Fig. 6c as a quasi-"experimental" data point. When L is shifted over the H-bond center to the right side, the negative second order term in eqn. (5) becomes so large that $J_{FL}{}^*$ goes through zero and becomes negative; eventually at very large F···H distances $J_{FL}{}^*$ and J_{FF} become zero. It is important to note that in the region of the sign change of $J_{FL}{}^*$, the heavy atom coupling J_{FF} is much larger than $J_{FL}{}^*$. The absence of scalar coupling of the proton across the hydrogen bond is, therefore, not caused by the purely electrostatic character of the hydrogen bond which manifests its covalent

character in the large J_{FF} values. The scalar spin coupling across a hydrogen bond arises to a large extent from the Fermi contact interaction,[40–42] which is typical for covalently bonded molecules.[25b,41,42] We note that the values are of the order of the geminal FCF couplings in saturated fluorocarbons (160–290 Hz), and even larger than the value of 95 Hz found for the fluorine-bridged anion, $[F_3B\text{-}F\text{-}BF_3]^-$.[43]

In Fig. 6d the hydron chemical shifts are plotted. The solid line was calculated using the equation

$$\delta(L) = \Delta_L(4p_{FL}p_{LF})^2 + \delta_L^\circ \quad (7)$$

for L = H, D with $\Delta_L = 8.9$ ppm, $\delta_L^\circ = 7.7$ ppm, where δ_L° represents the hydron chemical shift of free LF and $\Delta_L + \delta_L^\circ$ corresponds to the hydron chemical shift of FLF^-. In principle both δ_L° and Δ_L are isotope dependent, especially at $q_1 = 0$, but this effect was neglected. A comparison of eqn. (7) with eqn. (6) and also the corresponding solid lines in Fig. 6c and 6d indicate that both quantities, δ(L) and J_{FF} exhibit a similar dependence on q_1.

Finally, we plot in Fig. 6e the ^{19}F chemical shifts as function of q_1. The upper solid line in Fig. 6e was calculated using the equation

$$\delta_F = r\delta_{FL}{}^\circ p_{FL} + \delta_F{}^\infty p_{LF} \quad (8)$$

with $r = 1$, where $\delta_F{}^\infty$ and $\delta_{FL}{}^\circ$ represent the chemical shifts of the "free" hypothetical species F^- and LF according to Scheme 1. For the terminal fluorines these limiting values are correct. However, for the central fluorine only $\delta_F{}^\infty$ represents the correct limiting value, whereas the chemical shifts of the species L_2F^+ and L_2F^{2+} will be different from the value of LF. In order to take this difference into account, we introduced into eqn. (8) the correction factor r. We obtained the following values, $\delta_F{}^\infty = -100$ ppm and $\delta_{FH}{}^\circ = -210$ ppm from the upper curve in Fig. 6e, and the chemical shift correction factors $r = 1.3$ and 1.5 for L_2F^+ and L_2F^{2+} from the two lower curves in Fig. 6, adapted to fit the chemical shifts of the central fluorines in $F(HF)_2^-$ and $F(HF)_3^-$.

H/D isotope effects on $(FL)_nF^-$ clusters

FLF^-. In the case of the bifluoride ion, $q_1 = 0$ both for H and D isotopologs and eqn. (7) predicts the same ^1H (^2H) chemical shift for both anions. However, as indicated in Figs. 1 and 6d, FDF^- experiences a low-field shift as compared to FHF^-. This could be partially due to a shortening of the F···F distance caused by the smaller vibrational amplitude of D as compared to H. A value taking into account the mean amplitude of the stretching vibrations of 0.0058 Å was computed theoretically for the reduction of the F···F distance by deuteration.[36a] This value was taken into account in Fig. 6a, but the difference in the q_2 values of FHF^- and FDF^- is barely visible in this graph, in contrast to the corresponding hydron chemical shift difference in Fig. 6d. As a consequence, it is currently accepted that the major cause of the above-mentioned low-field shift of the deuteron in FDF^- as compared to the proton in FHF^- arises from the lower amplitude of stretch vibration, ν_3 (Σ_u) as depicted in Fig. 5b. This leads to a substantial value of the quadratic amplitude term $\Delta q_1{}^2$. In other words, the effect arises from the fact that D, compared to H, is more confined to the hydrogen bond center, where the deshielding exhibits a maximum value.[6,7,12,29] The high-field shift of F in FDF^- as compared to FHF^- needs further theoretical explanation.[44] Note, however, that the H/D isotope effects on the NMR chemical shifts are almost independent of the solvent polarity and temperature, and the symmetry of the ion is only slightly perturbed by intermolecular interactions.[6]

Table 4 Geometry of isotopologs of hydrogen bifluoride, dihydrogen trifluoride and trihydrogen tetrafluoride anions. Values for protonated anions are taken from ref. 25*a* and values for partially and fully deuterated isotopologs are calculated (see text)

Species	r_1/Å	r_2/Å	q_1/Å	q_2/Å
FHF^-	1.1495	1.1495	0	2.2990
FDF^-	1.1465	1.1465	0	2.2930
FHF^-HF	1.0142	1.3448	−0.1653	2.3589
$\underline{F}\underline{H}F^-DF$	1.0184	1.3368	−0.1592	2.3552
$FH\underline{F}^-D\underline{F}$	1.0088	1.3556	−0.1734	2.3644
$\underline{F}\underline{D}F^-DF$	1.0120	1.3490	−0.1685	2.3610
$\underline{F}\underline{H}F^-HF(HF)$	0.9800	1.4464	−0.2332	2.4264
$\underline{F}\underline{H}F^-HF(DF)$	0.9814	1.4396	−0.2291	2.4210
$\underline{F}H\underline{F}^-DF(DF)$	0.9814	1.4496	−0.2291	2.4210
$\underline{F}\underline{D}F^-HF(HF)$	0.9781	1.4555	−0.2387	2.4336
$\underline{F}\underline{D}F^-HF(DF)$	0.9790	1.4510	−0.2360	2.4300
$\underline{F}\underline{D}F^-DF(DF)$	0.9790	1.4510	−0.2360	2.4300
$\underline{F}\underline{H}F^-HF(HF)_2$	0.9610	1.5400	−0.2895	2.5010

$(FL)_2F^-$ and $(FL)_3F^-$. The refinement of the geometries of the protonated FHF^- hydrogen bond mentioned above was done as follows. It seemed to us that the experimental coupling constants J_{FF} are the most reliable quantities from which to obtain geometric information. A careful look at the experimental values of J_{FF} as a function of the calculated equilibrium values q_1 showed, unfortunately, small deviations from the solid lines calculated using eqn. (6). Therefore, we also fitted the same body of data to a polynomial function, resulting in a mathematical expression which exactly fits the data. As the parameters of this polynomial are not of physical interest, they are not discussed further. However, the polynomial allowed us to calculate the refined values of q_1 and hence of q_2 for the protonated clusters used in the preparation of Fig. 6. The refined data points are included in Table 4.

As the isotope effects are barely resolved in Fig. 6, they are illustrated in further detail in Figs. 7 and 8 as a function of the number m of H substituted by D: solid lines correspond to direct H/D isotope effects and broken lines to vicinal effects. Moreover, a schematic description of the geometric isotope effects is also shown in Fig. 9.

We note that the isotope effects on q_1 and on q_2 (Fig. 7b, c, f, g) are similar, which is not surprising in view of the correlation between both quantities which is linear in short intervals (Fig. 6a).

Complete H/D substitution leads to a reduction in J_{FF} for both anions. The corresponding geometric changes are in agreement with an increase in the F···F distances, *i.e.* q_2 values, of 0.0022 Å for deuterated $F(DF)_2^-$ and of 0.0035 Å for $F(DF)_3^-$ (Fig. 7b and f, Fig. 9). We note that this change is opposite to the change in FLF^-. The corresponding increases in the distance q_1 of D to the H-bond center are 0.0032 Å and 0.0027 Å (Table 4). Most interesting are the partially deuterated complexes. Single H/D substitution in a given hydrogen bond leads to a substantial increase in the F···F distance and a substantial asymmetrization, *i.e.* increase in the distance of the deuteron from the H-bond center. On the other hand, we find also a significant decrease in the F···F distance and a decrease in the hydron distance from the H-bond center when single H/D substitution occurs in a neighbouring H-bond. These single H/D effects are larger than the overall double HH/DD isotope effects. In the case of $F(DF)_3^-$ it seems that substitution of the last H by D exhibits no isotope effect, as illustrated in Fig. 7e to 7h, but we think that this effect is not real in view of the substantial margin of error of the changes in the coupling constants J_{FF}.

Let us discuss now the isotope effects on hydron-fluorine couplings J_{FL}*, included in the graphs of Fig. 7d and 7h. We note that the isotopic substitution pattern obtained resembles

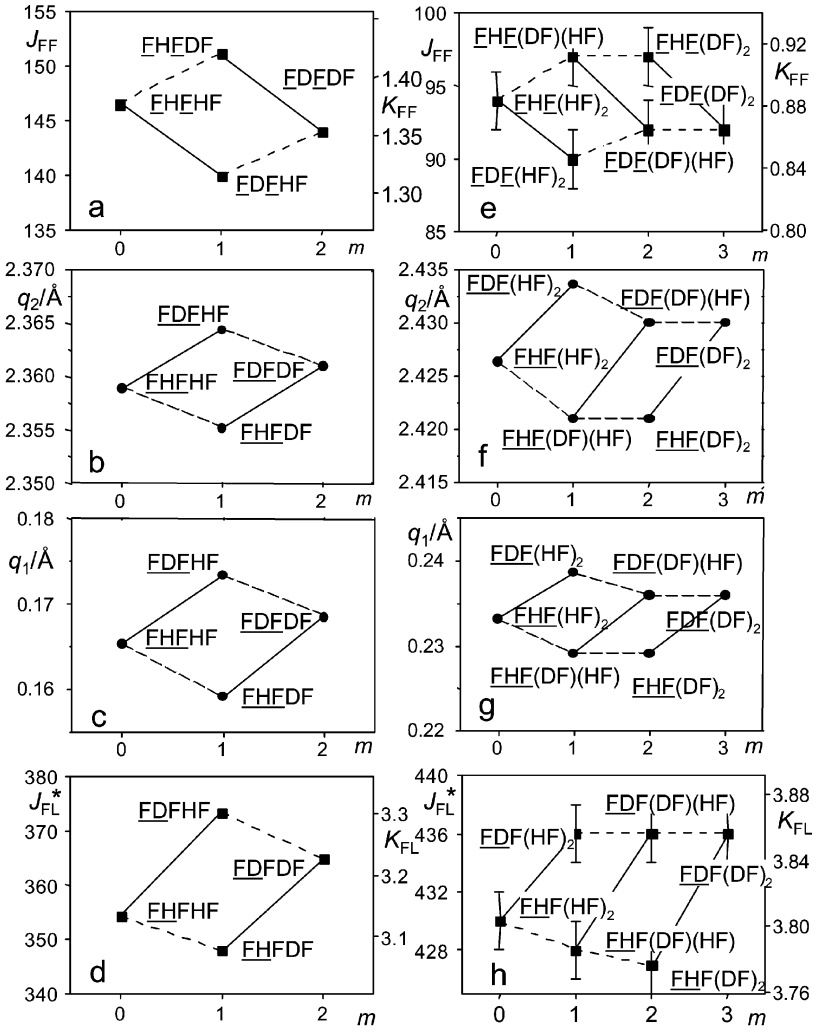

Fig. 7 Coupling constants and hydrogen bond coordinates of $(FL)_2F^-$ and $(FL)_3F^-$ (L = H,D) as a function of the number m of deuterons in the complexes. (a, e): scalar coupling constants J_{FF}/Hz and reduced couplings $K_{FF}/10^{20}$ T^2 J^{-1}. (b,c and f,g) hydrogen bond coordinates defined in Fig. 5, (d,h) fluorine–hydron couplings $J_{FL}^* = J_{FL}\gamma_H/\gamma_L$ defined in eqn. (4) as well as the corresponding reduced couplings $K_{FL}/10^{20}$ T^2 J^{-1}. Full lines depict the direct isotope effect, and the vicinal isotope effects are denoted by dotted lines. For further explanation see text.

the pattern obtained for q_1 and q_2. Again, we not only observe large primary isotope effects from $J_{FH} \equiv J_{\underline{F}\underline{H}FHF}$ to $J_{FD} \equiv J_{\underline{F}\underline{D}FHF}$ of about +19 Hz, as indicated by the solid lines, but also large vicinal isotope effects from $J_{\underline{F}\underline{H}FHF}$ to $J_{\underline{F}\underline{H}FDF}$ of about −6.4 Hz. To our knowledge, this is the first time that such isotope effects have been observed, at least for hydrogen-bonded systems. Because of the opposite sign of these effects the total isotope effect for the replacement of both H by D is only +12.6 Hz. On the other hand the $J_{\underline{F}\underline{H}FHF} - J_{\underline{F}\underline{D}FHF} = +6.6$ Hz, whereas $J_{\underline{F}\underline{H}FHF} - J_{\underline{F}\underline{H}FDF} = -4.6$ Hz leading to an overall effect of $J_{\underline{F}\underline{H}FHF} - J_{\underline{F}\underline{D}FDF} = +2.6$ Hz. For $F(LF)_3^-$ only the direct effects are substantial whereas the vicinal effects are smaller and not resolved within the margin of error. Unfortunately, we were not able to measure the coupling constants between D and F across the hydrogen bonds so that we are not able to include these effects in Fig. 7.

Let us now discuss the isotope effects on the chemical shifts, visualized in Fig. 8. Firstly, we note that the chemical shift changes of the terminal fluorines correspond to the predicted changes by the correlation curve of eqn. (8), indicating high field shifts for these nuclei when the bond lengths increase and the hydron is shifted away from the H-bond center.

However, the most surprising result is that the overall primary isotope effect on the hydron chemical shifts $\delta(F(\underline{D}F)_n^-) - \delta(F(\underline{H}F)_n^-)$ is positive and similar to that found for FLF^-, although in $F(LF)_n^-$ the F···F distances are increased by deuteration whereas they are decreased in FLF^-. This finding for $F(LF)_n^-$ (n = 2,3) is opposite to the prediction by the correlation curve of eqn. (7). This means that eqn. (7) is not valid to describe the details of this isotope effect. This effect was ascribed to the stronger confinement of the D in the H-bond as compared to H, *i.e.* $\Delta q_{1D}^2 < \Delta q_{1H}^2$, which dominates over the isotope effect on q_1. The same effect seems also to be responsible for the single vicinal H/D isotope effects on the hydron chemical shifts, which are larger than the direct effects as illustrated in Fig. 8a and d.

Finally, we discuss the isotope effects on the fluorine chemical shifts. The behaviour of the terminal fluorines is as expected, *i.e.* we find high-field shifts after deuteration which is in agreement with the correlation of Fig. 6e and a shortening of the fluorine–hydron distance. Similar isotope effects have been found previously for protonated pyridine.[26] By contrast, the isotope effect on the chemical shift of the central fluorine should be opposite and should lead to a low field shift because of a lengthening of the F···L distance after deuteration; however, the inverse is observed. This means that the central fluorine chemical shifts do not behave as predicted by the hydrogen bond correlation of eqn. (8). Here, we can only speculate again that the isotope effect on the chemical shift of the central fluorines is dominated by the anharmonic zero-point motions

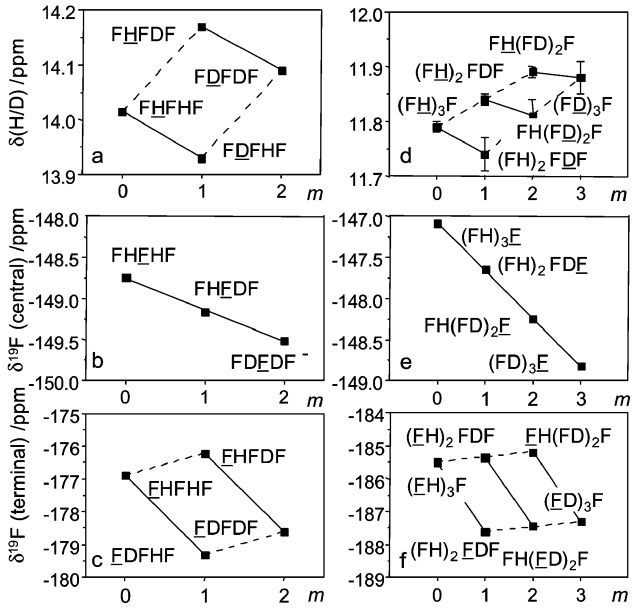

Fig. 8 Chemical shifts of three H/D isotopologs of the $(FH)_2F^-$ anion (a,b,c) and four isotopologs of the $(FH)_3F^-$ anion (d,e,f). *m* represents the number of deuterium atoms in hydrogen bonds. Full lines depict the direct isotope effect, while the vicinal isotope effects are denoted by dotted lines.

visualized in Fig. 5 which are not taken into account in the hydrogen bond correlations.

Finally, what are the systematic errors in the hydrogen bond geometries and the isotope effects on the latter made by the above analysis? There are many sources: (i) the quality of the *ab initio* calculations used to calculate the equilibrium geometries, (ii) the neglect of solvent effects, (iii) the assumption that the equilibrium geometries correspond to those of the deuterated complexes, *i.e.* the neglect of the vibrational anharmonicity in the latter, (iv) the assumption that the parameters of the various hydrogen bond correlations are the same for the protonated and deuterated complexes. It is difficult to estimate the contributions of these sources. However, we estimate that many of these effects cancel in the values of the H/D isotope effects on the hydrogen bond geometries, whereas the effects are large in the absolute values of these coordinates.

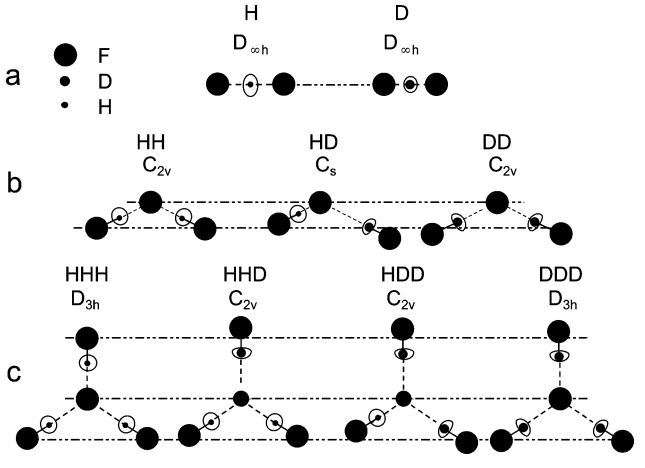

Fig. 9 Schematic representation of changes in effective (vibrationally averaged) geometry of the FHF^-, $(FH)_2F^-$ and $(FH)_3F^-$ anions resulting from successive H/D replacement.

The error of these absolute values can be estimated assuming that for any vibrational AH stretching coordinate q the difference between the true value q_L and the equilibrium mass-independent value $q(\mathrm{eq})$ is proportional to the square of the vibrational energy and hence proportional to the inverse mass of the hydrogen isotope, *i.e.* $q_L - q_L(\mathrm{eq}) \propto {E_{vib}}^2 \propto 1/m_L$. It is then straightforward to write

$$q_H = q(\mathrm{eq}) + 2(q_H - q_D) \text{ and } q_D = q(\mathrm{eq}) + (q_H - q_D) \quad (9)$$

because the equilibrium distance $q(\mathrm{eq})$ is the same for H and D. By contrast, we assumed in the above analysis that

$$q_H = q_H(\mathrm{eq}) + (q_H - q_D) \text{ and } q_D = q_H(\mathrm{eq}) \quad (10)$$

Thus, it could be that the hydrogen bond geometries reported here for the protonated complexes refer in fact to the deuterated complexes; doubling of the isotope effect which we assume to be less affected by systematic errors, leads then to the "doubly" refined geometries of the protonated complexes. However, eqn. (9) is only an estimate, and was, therefore, not used in the above data analysis. Nevertheless, it provides a feeling for the magnitude of the absolute errors of q_1 and q_2, which is then of the order of the isotope effects on these quantities, whereas the error of the latter is much smaller.

Sum rules

We come now to the, at first sight, surprising symmetry of the parallelograms in Figs. 7 and 8. According to Tables 2 and 3, for a given quantity, NMR parameter or hydrogen bond coordinate V, these findings indicate that

$$V_H(\mathrm{HH}) + V_D(\mathrm{DD}) = V_H(\mathrm{HD}) + V_D(\mathrm{DH}) \quad (11)$$

$$V_H(\mathrm{HHH}) + V_D(\mathrm{DDD}) = V_H(\mathrm{HDD}) + V_D(\mathrm{HHD}) = V_H(\mathrm{HHD}) + V_D(\mathrm{HDD}), \quad (12)$$

where V_H refers to an FH···F bond and V_D to an FD···F bond. In other words, the resulting effect of total (double or triple) deuteration corresponds approximately to the algebraic sum of the direct (or one-bond) and the vicinal isotope (or secondary) effects. Or: for every parameter, the average value over all isotopologs belonging to a definite local point group is constant.

We note that the sum rules found in this paper for NMR parameters and H-bond geometries coincide with the well known sum rules for vibrational frequencies.[45] We also note that sum rules have been previously established, for example for the ^{13}C chemical shift of methane H/D isotopologs[19a] and of ammonia,[19b] but deviations were observed for ammonium.[19c] The isotopic sum rules can facilitate considerably the assignment of spectral lines to given H/D isotopologs when scalar couplings across hydrogen bonds are absent, *e.g.* in the case of systems of hydrogen-bonded complexes of the OHO type. The problem of line identification is especially important for isotopic modifications of hydrogen-bonded systems which cannot be studied separately but only as an equilibrium mixture. In addition, the rule provides grounds for the method of determination of the composition of hydrogen-bonded associates using the multiplicity of isotopic splitting proposed in ref. 28. In particular, it excludes the possibility of occasional coincidence of several lines in such an isotopic multiplet.

As the sum rules are valid for so many different quantities they arise most probably, from a similar origin. On the other hand, the sum rules as well as the analogous product rules for vibrational frequencies were derived in harmonic approximation, whereas the isotope effects on the NMR parameters and on H-bond geometries are essentially caused by an anharmonic effect. A consideration of this problem in terms of perturbation theory will be given elsewhere.

Conclusions

1. The low temperature NMR technique in the slow exchange regime provides the possibility of resolving spectra of H/D isotopologs of ionic clusters involving several hydrogen bonds.

2. Using hydrogen bond correlations established previously the changes in the hydrogen bond geometries upon deuteration could be estimated. Isotope effects on the hydron delocalization in the hydrogen bonds could be qualitatively estimated from the hydron chemical shifts.

3. It has been found that the anti-cooperative mutual influence of hydrogen bonds in ionic clusters, $(FH)_nF^-$ ($n = 2,3$) leads to different signs of the direct and vicinal H/D isotope effects on NMR chemical shifts and scalar coupling constants. Whereas direct effects are strongly affected by the isotope effects on the hydron delocalization the vicinal effects can be explained mainly in terms of isotope effects on average atom positions.

4. A simple qualitative treatment of the observed vicinal isotope effects is given in terms of anharmonic changes in the effective hydrogen bond lengths caused by H/D substitution in a neighbouring hydrogen bond.

5. An empirical sum rule for NMR parameters and geometries of H/D isotopologs is proposed which can be of help in assigning spectral lines to different isotopologs.

Acknowledgements

The authors are grateful to Dr D. N. Shchepkin for his kind interest and helpful discussions. This work has been supported by the Deutsche Forschungsgemeinschaft, the Russian Foundation for Basic Research, grants 00-03-32923 and 02-03-32668, and the Fonds der Chemischen Industrie, Frankfurt.

References

1 P. E. Hansen, *Prog. NMR Spectrosc.*, 1988, **20**, 207.
2 C. J. Jameson, in *Encyclopedia of NMR*, ed. D. M. Grant and R. K. Harris, New York, 1996, vol. 4.
3 C. J. Jameson and H. J. Osten, *J. Am. Chem. Soc.*, 1986, **108**, 2497.
4 N. N. Shapetko, Yu. S. Bogachev, I. L. Radushnova and D. N. Shigorin, *Dokl. Akad. Nauk SSSR*, 1976, **231**, 409.
5 M. D. Fenn and E. Spinner, *J. Phys. Chem.*, 1984, **88**, 3993.
6 P. Schah-Mohammedi, I. G. Shenderovich, C. Detering, H.-H. Limbach, P. M. Tolstoy, S. N. Smirnov, G. S. Denisov and N. S. Golubev, *J. Am. Chem. Soc.*, 2000, **122**, 12 878.
7 L. J. Altman, D. Laungani, G. Gunnarsson, H. Wennerström and S. Forsen, *J. Am. Chem. Soc.*, 1978, **100**, 8264.
8 S. Bolvig, P. E. Hansen, H. Morimoto, D. Wemmer and P. Williams, *Magn. Reson. Chem.*, 2000, **38**, 525.
9 H. Benedict, H. H. Limbach, M. Wehlan, W. P. Fehlhammer, N. S. Golubev and R. Janoschek, *J. Am. Chem. Soc.*, 1998, **120**, 2939.
10 T. Dziembowska and Z. Rozwadowski, *Curr. Org. Chem.*, 2001, **5**, 289.
11 M. Rospenk, A. Koll and L. Sobczyk, *Chem. Phys. Lett.*, 1996, **261**, 283.
12 G. Gunnarsson, H. Wennerström, W. Egan and S. Forsen, *Chem. Phys. Lett.*, 1976, **38**, 96.
13 C. Engdahl, A. Gogoll and U. Edlund, *Magn. Reson. Chem.*, 1991, **29**, 54.
14 M. V. Vener, *Chem. Phys.*, 1992, **166**, 311.
15 N. S. Golubev, S. N. Smirnov, V. A. Gindin, G. S. Denisov, H. Benedict and H.-H. Limbach, *J. Am. Chem. Soc.*, 1994, **116**, 12 055.
16 C. L. Perrin and J. B. Nielson, *J. Am. Chem. Soc.*, 1997, **119**, 12 734.
17 N. M. Sergeyev, in *Encyclopedia of NMR*, ed. D. M. Grant and R. K. Harris, New York, 1996, vol. 1.
18 C. J. Jameson, A. C. de Dios and A. K. Jameson, *J. Chem. Phys.*, 1991, **95**, 9042.
19 (*a*) P. Lazzaretti, R. Zanasi, A. J. Sadlej and W. T. Raynes, *Mol. Phys.*, 1987, **62**, 605; (*b*) W. M. Litchman, M. Alei and A. E. Florin, *J. Chem. Phys.*, 1969, **50**, 1897; (*c*) P. E. Hansen and A. Lycka, *Acta Chem. Scand.*, 1989, **43**, 222.
20 A. D. Buckingham and R. M. Olegario, *Mol. Phys.*, 1997, **92**, 773.
21 R. D. Wigglesworth, W. Raynes, S. Kirpekar, J. Oddershede and S. Sauer, *J. Chem. Phys.*, 2000, **112**, 736.
22 R. D. Wigglesworth, W. Raynes, S. Kirpekar, J. Oddershede and S. Sauer, *J. Chem. Phys.*, 2000, **112**, 3735; R. D. Wigglesworth, W. Raynes, S. Kirpekar, J. Oddershede and S. Sauer, *J. Chem. Phys.*, 2001, **114**, 9192, erratum.
23 J. E. Del Bene, M. J. T. Jordan, S. A. Perera and R. J. Bartlett, *J. Phys. Chem. A*, 2001, **105**, 8399.
24 N. S. Golubev and G. S. Denisov, *J. Mol. Struct.*, 1992, **270**, 263.
25 (*a*) I. G. Shenderovich, S. N. Smirnov, G. S. Denisov, V. A. Gindin, N. S. Golubev, A. Dunger, R. Reibke, S. Kirpekar, O. L. Malkina and H.-H. Limbach, *Ber. Bunsen-Ges. Phys. Chem.*, 1998, **102**, 422; (*b*) H. Benedict, I. G. Shenderovich, O. L. Malkina, V. G. Malkin, G. S. Denisov, N. S. Golubev and H.-H. Limbach, *J. Am. Chem. Soc.*, 2000, **122**, 1979.
26 S. N. Smirnov, N. S. Golubev, G. S. Denisov, H. Benedict, P. Schah-Mohammedi and H.-H. Limbach, *J. Am. Chem. Soc.*, 1996, **118**, 4094.
27 N. S. Golubev, S. N. Smirnov, P. Schah-Mohammedi, I. G. Shenderovich, G. S. Denisov, V. A. Gindin and H.-H. Limbach, *Zh. Obshch. Khim.*, 1997, **67**, 1150; N. S. Golubev, S. N. Smirnov, P. Schah-Mohammedi, I. G. Shenderovich, G. S. Denisov, V. A. Gindin and H.-H. Limbach, *Russ. J. Gen. Chem.*, 1997, **67**, 1082.
28 C. Detering, P. M. Tolstoy, N. S. Golubev, G. S. Denisov and H.-H. Limbach, *Dokl. Akad. Nauk*, 2001, **379**, 353; C. Detering, P. M. Tolstoy, N. S. Golubev, G. S. Denisov and H.-H. Limbach, *Dokl. Phys. Chem.*, 2001, **379**, 191.
29 F. Y. Fujiwara and J. S. Martin, *J. Am. Chem. Soc.*, 1974, **96**, 7625.
30 S. A. Perera and R. J. Bartlett, *J. Am. Chem. Soc.*, 2000, **122**, 1231.
31 I. G. Shenderovich, A. P. Burtsev, G. S. Denisov, N. S. Golubev and H.-H. Limbach, *Magn. Reson. Chem.*, 2001, **39**, S91.
32 J. E. Del Bene and I. Shavitt, *J. Mol. Struct. (THEOCHEM)*, 1991, **234**, 499.
33 D. Mootz and D. Boenigk, *Z. Anorg. Allg. Chem.*, 1987, **544**, 159.
34 R. R. Lovelace and K. M. Harmon, *J. Mol. Struct.*, 1989, **193**, 247.
35 W. D. Chandler, K. E. Johnson and J. L. E. Campbell, *Inorg. Chem.*, 1995, **34**, 4943.
36 (*a*) J. Almlöf, *Chem. Phys. Lett.*, 1972, **17**, 49; (*b*) K. Kawaguchi and E. Hirota, *J. Chem. Phys.*, 1987, **87**, 6838; (*c*) K. Kawaguchi and E. Hirota, *J. Mol. Struct.*, 1995, **352/353**, 389.
37 Ph. Lorente, I. G. Shenderovich, G. Buntkowsky, N. S. Golubev, G. S. Denisov and H.-H. Limbach, *Magn. Reson. Chem.*, 2001, **39**, S18.
38 (*a*) Th. Steiner and W. Saenger, *Acta Crystallogr. Sect. B*, 1994, **50**, 348; (*b*) Th. Steiner, *J. Chem. Soc. Chem. Commun.*, 1995, 1331; (*c*) P. Gilli, V. Bertolasi, V. Ferretti and G. Gilli, *J. Am. Chem. Soc.*, 1994, **116**, 909; (*d*) Th. Steiner, *J. Phys. Chem. A*, 1998, **102**, 7041.
39 The value of 220 Hz corresponds to the maximum of the estimated solid line in Fig. 3c of ref. 25*a*.
40 A. Bagno, *Chem. – Eur. J.*, 2000, **6**, 2925.
41 W. D. Arnold and E. Oldfield, *J. Am. Chem. Soc.*, 2000, **122**, 12 835.
42 F. Löhr, S. G. Mayhew and H. Rüterjans, *J. Am. Chem. Soc.*, 2000, **122**, 9289.
43 J. S. Hartman and P. Stilbs, *J. Chem. Soc., Chem. Commun.*, 1975, 566.
44 N. S. Golubev and G. S. Denisov, in preparation.
45 E. B. Wilson, J. C. Decius and P. C. Cross, *Molecular Vibrations*, McGraw-Hill, London, 1955.